Proceedings of Symposia in Applied Mathematics

Accuracy of modeling error estimates for discrete velocity models

K. C. Assi and M. Laforest

Abstract. We study the spatial difference in L^1 between two solutions of different discrete velocity models in one space dimension using techniques developed by Ha and Tzavaras. We assume that the second (fine) model is obtained by adding new velocities to the first (coarse) model, although the collision operators can be completely different. The 1-D discrete velocity models studied here include projections of n-D models, as described by Beale. With the help of numerical experiments, we show that the error estimator previously developed by the authors gives an accurate a posteriori error estimate. We also give a general discussion of hierarchies of discrete velocity models and of their constructibility.

1. Introduction

Consider two solutions $f_n(x,t)$ and $\bar{f}_m(x,t)$ of two different discrete velocity models (DVM) in 1-D :

$$\left.\begin{array}{rcl} \partial_t f_n + v_n \partial_x f_n &=& \sum_{i,j=1}^{N} B_n^{ij} f_i f_j \\ f_n(x,0) &=& f_{n,0}(x) \end{array}\right\} n = 1,\ldots,N \tag{1.1}$$

$$\left.\begin{array}{rcl} \partial_t \bar{f}_m + \bar{v}_m \partial_x \bar{f}_m &=& \sum_{i,j=1}^{\bar{N}} \bar{B}_m^{ij} \bar{f}_i \bar{f}_j \\ \bar{f}_m(x,0) &=& \bar{f}_{m,0}(x) \end{array}\right\} m = 1,\ldots,\bar{N} \tag{1.2}$$

where the constants B_k^{ij} and $\bar{B}_k^{ij}$ must satisfy certain constraints (e.g. see Section 2) and we assume $N < \bar{N}$ and $v_n = \bar{v}_n$. If one interprets the first equation (1.1) as a rough scale approximation of the collision dynamics of a dilute gas and equation (1.2) as a much finer, but more difficult to compute, approximation of the collision dynamics, then it is natural to ask when are the solutions to the coarse model (1.1) sufficiently accurate? Adapting the techniques used by Ha and Tzavaras [**H**], in particular their quadratic functional, Assi and Laforest [**A**] have shown that the

1991 *Mathematics Subject Classification.* Primary 74A25, 35L50; Secondary 65M15.

Key words and phrases. stability, modeling error, discrete velocity model.

The first author was supported in part by NSERC and the École Polytechnique de Montréal.

The first author was supported in part by NSERC and CFI Canada.

spatial difference in $L^1(\mathbb{R})$ between the two solutions is bounded by the norm in $L^1([0,T]\times\mathbb{R})$ of the *residual* of the coarse approximation. This leads to a *computable* error estimate that can rigorously determine when a coarse model resolves the fine scale dynamics to within a prescribed tolerance without having to compute the (expensive) fine scale solution.

The purpose of this paper is to provide numerical confirmation of the efficiency of the error estimator presented in [**A**] and of the necessity of the conditions under which it was derived. We also describe a class of hierarchies of DVMs in several space dimensions, and use these to construct a hierarchy of 1-D DVMs on which to test the error estimator. The tests indicate that not all conditions appear to be necessary, as was first suggested by Ha and Tzavaras [**H**].

The main application for such a computable error estimate appears to be to the efficient approximate solution the Boltzmann equation with the help of discrete velocity models (DVM). DVMs are used as the basis for several numerical schemes, such as the Random Discrete Velocity Model of Illner and Rjasanow [**I**], a DVM-based solver for the Boltzmann-BGK equation [**J**] and an adaptive DVM for the shallow water equations [**K**]. Unfortunately, DVM-based schemes did not possess rigorous estimators to adapt the discretization in velocity space, in contrast to methods based on Fourier transforms on velocity space where truncation was always available and easily computable. The numerical results in this paper justify the use of the error estimate in [**A**] as the basis for adaptive DVM-based schemes. This is the subject of ongoing work [**B**].

The paper is organized as follows. Section 2 contains preliminaries on the class of 1-D DVMs studied in this paper. and a complete description of the error estimator in [**A**]. Section 3 discusses hierarchies of DVM and the final section contains numerical results that confirm the efficiency of the error estimator.

2. Error estimate for 1-D discrete velocity models

In this section, we describe the structural hypothesis that we impose on 1-D models (1.1), (1.2) as well as the well-posedness theory for these systems. The results treated here are largely taken from [**D, H**]. First proposed in 2 and 3-D as discretizations of Boltzmann's equation, Beale formalized the notion of 1-D DVMs in [**D**], which could occur as projections of n-D models. The complexity of 1-D models is attributable to the fact that projections of DVMs don't preserve energy.

Suppose that at each point x in some domain $\Omega \subset \mathbb{R}$, not necessarily bounded, and at each time t, the velocities of the particles located at (x,t) can only belong to the finite set $v_1, v_2, \ldots, v_n$. Suppose that $f_i(x,t)$ represents the density of particles at (x,t) with velocity v_i. Under classical statistical hypothesis, the rate of creation/destruction of particles with speed v_n at (x,t) by means of binary collisions is given by the so-called *collision kernel* :

$$Q_n(\mathbf{f})(x,t) := \sum_{i,j=1}^{N} B_n^{ij} f_i(x,t) f_j(x,t). \tag{2.1}$$

The coefficients B_n^{ij} determine the rate of production of particles with speed v_n occurring from the collisions between particles with speeds v_i and v_j. Basic microscopic considerations provide the following set of contraints on the coefficients

$$B_k^{ij} = B_k^{ji} \tag{2.2}$$

$$B_k^{ij} \geq 0 \text{ if } k \neq i \text{ and } k \neq j, \tag{2.3}$$

$$\left|B_k^{ij}\right| \leq B^* \quad \text{for some positive } B^*. \tag{2.4}$$

The other conditions we impose on 1-D models are slightly more complex.

We suppose there exists *masses* $\nu_n \geq 1$ with respect to which we express the analogue of conservation of mass and momentum

$$\sum_{k=1}^{N} \nu_k B_k^{ij} = 0, \qquad \sum_{k=1}^{N} v_k \nu_k B_k^{ij} = 0. \tag{2.5}$$

For projections, the term mass is a misnomer since it is simply the number of n-D velocities that are symmetric with respect to the projection, e.g. Section 3. These projected models are not necessarily strictly hyperbolic but, following [**H**], we nonetheless assume

$$v_1 < v_2 < \cdots < v_N. \tag{2.6}$$

Numerical results presented here indicate that strict hyperbolicity might not be necessary, as was remarked in [**H**]. Finally, we also suppose that for these models,

$$\begin{aligned} &\text{if } B_i^{ii} < 0 \text{ then there is for some } i = i_1, i_2, \ldots, i_r, \text{ for which} \\ &B_{i_{k+1}}^{i_k i_k} > 0 \text{ but } B_{i_r}^{i_r i_r} = 0. \end{aligned} \tag{2.7}$$

In a context where (1.1) is a coarse approximation of the fine model (1.2), one would expect some relation between the collision kernels. Very specific hierarchies of DVMs are constructed in Section 3 but for the purposes of estimating the modeling error, the only hypothesis we impose is that

$$v_i = \bar{v}_i, \qquad \nu_i = \bar{\nu}_i, \qquad i = 1, \ldots, N. \tag{2.8}$$

The existence theory for 1-D systems satisfying (2.2)-(2.7) has been extensively studied. In 1-D, one can find existence results for small [**L**] and large [**M**] L^1 initial data. Asymptotic results were considered [**D**], uniform bounds are available for solutions with data in $L^1 \cap L^\infty$, as well as stability results for initial data in L^1 [**H**]. The usual notion of a solution to (1.1) is the following.

Definition 2.1. We say that $\mathbf{f} = (f_1, \ldots, f_N)^T \in C([0,T], L^1(\mathbb{R})^N)$ is a *mild solution* of (1.1) if for $t \in [0,T]$ and a.a. $x \in \mathbb{R}$ and all $i = 1, \ldots, N$, the functions f_i satisfy

$$f_i(x,t) = f_{i,0}(x) + \int_0^t Q_i(\mathbf{f})\big(x - v_i(t-\tau)\big)\, d\tau. \tag{2.9}$$

As far as we are concerned, the existence result we need is the following, first proved by [**D, F**], and taken in this form from [**H**].

Theorem 2.2 ([**D, F**]). *Suppose that the system* (1.1) *satisfies conditions* (2.2)-(2.7) *and that the initial conditions* $f_{n,0}$ *are nonnegative and belong to* $L^1(\mathbb{R}) \cap$

$L^\infty(\mathbb{R})$. *Then there exists a unique nonnegative mild solution* $\mathbf{f} = (f_1, \dots, f_N)^T$ *of* (1.1) *such that for any* $T > 0$*, any* $i = 1, \dots, N$*,*

$$f_i \in C\big([0,T], L^1(\mathbb{R})\big) \cap L^\infty(\mathbb{R} \times [0,T]),$$

and $Q_i(\mathbf{f}) \in L^1(\mathbb{R} \times \mathbb{R}^+)$.

In practice, the objective is to estimate the difference between a previously computed solution $\mathbf{f}$ of (1.1) and an uncomputed solution $\bar{\mathbf{f}}$ of (1.2). The quantity that can most naturally account for this difference is the *residual*

$$R_m(\mathbf{f}) := \begin{cases} Q_m(\mathbf{f}) - \bar{Q}_m(\mathbf{f}), & 1 \le m \le N, \\ -\bar{Q}_m(\mathbf{f}), & N+1 \le m \le \bar{N}. \end{cases} \tag{2.10}$$

The key point is that the residual does not depend on $\bar{\mathbf{f}}$. The following version of the residual can take into account the contributions from all the components

$$\mathcal{R}(\mathbf{f})(t) = \sum_{m=1}^{\bar{N}} \int_{\mathbb{R}} \bar{\nu}_m \big| R_m(\mathbf{f})(x) \big| \, dx. \tag{2.11}$$

Theorem 2.3. *Consider differential equations* (1.1) *and* (1.2) *satisfying the hypothesis* (2.2) *through to* (2.8). *Suppose that* $\mathbf{f}$ *and* $\bar{\mathbf{f}}$ *are mild solutions in* $C([0,T], L^1(\mathbb{R}))$ *to respectively* (1.1) *and* (1.2) *with positive initial data* $\mathbf{f}_0$ *and* $\bar{\mathbf{f}}_0$ *in* $L^1(\mathbb{R}) \cap L^\infty(\mathbb{R})$. *Then there exists positive constants* c_1 *and* c_2*, independent of* $\mathbf{f}$ *and* $\bar{\mathbf{f}}$ *but dependent on* $\mathbf{f}_0, \bar{\mathbf{f}}_0, Q, \bar{Q}, v_n, \bar{v}_n, \nu_n, \bar{\nu}_n$*, such that for all* T

$$\big\| \mathbf{f}(\cdot, T) - \bar{\mathbf{f}}(\cdot, T) \big\|_{L^1(\mathbb{R})} \le c_1 \big\| \mathbf{f}_0 - \bar{\mathbf{f}}_0 \big\|_{L^1(\mathbb{R})} + c_2 \int_0^T \mathcal{R}(\mathbf{f})(s) \, ds. \tag{2.12}$$

In Section 4, the tightness of this bound will be studied and its dependence on the hypothesis (2.2)-(2.8) will also be evaluated.

3. Hierarchies of n-D discrete velocity models

In this section, we give a construction of hierarchies of DVMs in n-D. This topic has been touched upon in the monograph [**G**], and also in the context of chemically reacting species [**E**]. The general construction given here is used to construct a hierarchy on which to perform the numerical experiments of Section 4. The presentation given here is by no means the most general but it does indicate how rich hierarchies of DVMs can be.

In n-D, consider a DVM with M velocities

$$\mathbf{u}_1, \mathbf{u}_2, \dots, \mathbf{u}_M \in \mathbb{R}^n, \tag{3.1}$$

all masses equal to 1, and involving collisions $(i,j) \to (k,l)$ which satisfy conservation of momentum and energy

$$\mathbf{u}_i + \mathbf{u}_j = \mathbf{u}_k + \mathbf{u}_l, \qquad |\mathbf{u}_i|^2 + |\mathbf{u}_j|^2 = |\mathbf{u}_k|^2 + |\mathbf{u}_l|^2. \tag{3.2}$$

The explicit construction of a continuous family of extensions of DVMs is more natural if it is written in terms of *transition probabilities* p^{ij}_{kl} rather than the transition rates B^{ij}_k. The transition probability p^{ij}_{kl} is the probability that a collision between particles with incoming speeds $\mathbf{u}_i, \mathbf{u}_j$ result in particles with outgoing speeds $\mathbf{u}_k, \mathbf{u}_l$. Basic mechanical considerations imply that the transition probabilities satisfy

(*i*) $\sum_{k,l} p^{ij}_{kl} = 1$;

(ii) $p^{ij}_{kl} = p^{ij}_{lk} = p^{ji}_{kl}$;
(iii) $p^{in}_{im} = 0$ if $n \neq m$;
(iv) $p^{ii}_{kl} = p^{kl}_{ii}$ if $k \neq i$ or $l \neq i$;
(v) $p^{ij}_{kl} = 0$ if the collision does not conserve momentum and energy ;
(vi) $p^{ij}_{kl} = p^{kl}_{ij}$;

Dimensional analysis shows that the DVM evolves according to

$$\partial_t f_i + \mathbf{u}_i \cdot \nabla_x f_i = \sum_{j,k,l=1}^{M} A^{ij}_{kl}\Big(f_k f_l - f_i f_j\Big),$$

for $A^{ij}_{kl} := \frac{C}{\varepsilon} p^{ij}_{kl} |\mathbf{u}_i - \mathbf{u}_j|$, where ε is the mean free path and C is some constant independent of i, j, k, l. Using some algebra, it can be shown that the transition rates are

$$B^{ij}_k = \sum_{l=1}^{M} A^{kl}_{ij} - \frac{1}{2}\sum_{m,n=1}^{M} A^{mn}_{ij}\delta_{ki} - \frac{1}{2}\sum_{m,n=1}^{M} A^{mn}_{ij}\delta_{jk}. \tag{3.3}$$

In the n-D setting, the transition rates so defined satisfy (2.2)-(2.5) (with ν_n replaced by 1), as well as an obvious analog for energy conservation.

If one is to consider an extension of an n-D DVM, it is natural to suppose that the transition probabilities in both models should be the same when they involve transverse interactions among the initial set of particles. The objective will be to construct an extension that satisfies this condition and such that the "total" rate of collisions is the same. Below, we will need the following sets of pairs of indices

$$D = \{1,\dots,M\}\times\{1,\dots,M\}, \quad \bar{D} = \{1,\dots,\bar{M}\}\times\{1,\dots,\bar{M}\}, D^* = \bar{D}\setminus D.$$

Definition 3.1. We say that a DVM $\{\bar{p}^{ij}_{kl}\}$ is a *compatible* extension of a DVM $\{p^{ij}_{kl}\}$ if it is defined for a set of velocities that include (3.1) and if $\bar{p}^{ij}_{kl} = p^{ij}_{kl}$ when $(i,j),(k,l) \in D$ but $(i,j) \neq (k,l),(l,k)$.

Lemma 3.2. *Suppose that the collision model $\{p^{ij}_{kl}\}$ satisfies the conditions (i)-(vi) for a set of particles with speeds* (3.1) *and equal masses. Suppose that the extended velocities $\bar{\mathbf{u}}_1, \dots \bar{\mathbf{u}}_{\bar{M}}$ are such that $\mathbf{u}_i = \bar{\mathbf{u}}_i, i = 1,\dots,M$. Let $\{\lambda^{ij}\}_{(i,j)\in D}$, $\{\Omega^{ij}_{kl}\}_{(i,j,k,l)\in\bar{D}\times D^*}$ be constants such that $\lambda^{ij}\in[0,1]$ and $\Omega^{ij}_{kl}\in[0,1]$ satisfies*

(A.1) $\sum_{(k,l)\in D^*} \Omega^{ij}_{kl} = 1$;
(A.2) $\Omega^{ij}_{kl} = \Omega^{ji}_{kl} = \Omega^{ji}_{lk}$;
(A.3) $\Omega^{in}_{im} = 0$ *if $n \neq m$;*
(A.4) $\Omega^{ij}_{kl} = 0$ *if the collision does not conserve momentum and energy ;*

and define the coefficients $\bar{p}^{ij}_{kl}$ according to :

(B.1) *if $(i,j) \in D$*

$$\bar{p}^{ij}_{kl} := \begin{cases} (1-\lambda^{ij})p^{ij}_{ij} & \textit{if } (k,l) = (i,j), \\ p^{ij}_{kl} & \textit{if } (k,l) \in D\setminus\{(i,j),(j,i)\}, \\ \lambda^{ij} p^{ij}_{ij}\Omega^{ij}_{kl} & \textit{if } (k,l)\in D^*, \end{cases}$$

(B.2) *if $(i,j) \in D^*$*

$$\bar{p}^{ij}_{kl} := \begin{cases} (1-\lambda^{ij}) & \textit{if } (i,j) = (k,l), \\ \lambda^{ij}\Omega^{ij}_{kl} & \textit{if } (k,l) \neq (i,j). \end{cases}$$

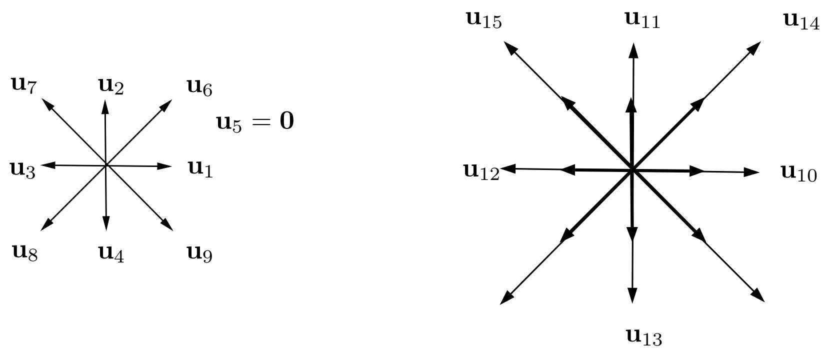

FIGURE 1. Velocities in the coarse DVM (left) and the fine DVM (right).

Under these conditions, the coefficients $\bar{p}^{ij}_{kl}$ *are transition probabilities for a DVM satisfying (i)-(vi). This new DVM is a compatible extension of* (1.1).

PROOF. To demonstrate (i) when $(i,j) \in D$, use properties (A.3), (B.1) and (B.2) to compute the following.

$$\begin{aligned}\sum_{(k,l)\in\bar{D}} \bar{p}^{ij}_{kl} &= \bar{p}^{ij}_{ij} + \sum_{\substack{(k,l)\in D\\(k,l)\neq(i,j)}} \bar{p}^{ij}_{kl} + \sum_{(k,l)\in D^*} \bar{p}^{ij}_{kl}\\ &= (1-\lambda^{ij})p^{ij}_{ij} + \sum_{\substack{(k,l)\in D\\(k,l)\neq(i,j)}} p^{ij}_{kl} + \lambda^{ij}p^{ij}_{ij}\sum_{(k,l)\in D^*}\Omega^{ij}_{kl}\\ &= p^{ij}_{ij} - \lambda^{ij}p^{ij}_{ij} + \sum_{\substack{(k,l)\in D\\(k,l)\neq(i,j)}} p^{ij}_{kl} + \lambda^{ij}p^{ij}_{ij} = 1.\end{aligned}$$

A similar argument demonstrates (i) when $(i,j) \in D^*$. Properties $(ii)-(vi)$ follow immediately from (A.1)-(B.2). □

The construction described above is rich in the sense that the parameters $\lambda^{ij} \in [0,1]$ are arbitrary. On the other hand, the Ω^{ij}_{kl} control the transition probabilities for the extended set of velocities. The compatibility is continuous and uniform in the following sense.

COROLLARY 3.3. *If all the coefficients* $\lambda^{ij} \to 0$, *then for* $(i,j) \in D$,

$$\bar{p}^{ij}_{kl} \to \begin{cases} p^{ij}_{kl} & \text{if } (i,j),(k,l) \in D\\ 0 & \text{otherwise.}\end{cases}$$

Moreover, for all (k,l) *and* $(m,n) \neq (i,j),(j,i)$ *and* $\lambda^{ij} \neq 0$, *the ratio* $\bar{p}^{ij}_{kl}/\bar{p}^{ij}_{mn}$ *is constant and independent of* λ^{ij}.

EXAMPLE 3.4. We now present an example of two nested 2-D DVMs; the coarse DVM involving 9 velocities and the fine DVM involving 17 velocities. The velocities in the coarse DVM are

$$\mathbf{u}_1 = (1,0),\quad \mathbf{u}_2 = (0,1),\quad \mathbf{u}_3 = -\mathbf{u}_1,\quad \mathbf{u}_4 = -\mathbf{u}_2,\qquad \mathbf{u}_5 = (0,0),$$
$$\mathbf{u}_6 = (1,1),\quad \mathbf{u}_7 = (-1,1),\quad \mathbf{u}_8 = -\mathbf{u}_6,\quad \mathbf{u}_9 = -\mathbf{u}_7,$$

and those in the fine model are

$$\mathbf{u}_{10} = (2,0), \quad \mathbf{u}_{11} = (0,2), \quad \mathbf{u}_{12} = -\mathbf{u}_{10}, \quad \mathbf{u}_{13} = -\mathbf{u}_{11},$$
$$\mathbf{u}_{14} = (2\sqrt{2}, 2\sqrt{2}), \quad \mathbf{u}_{15} = (-2\sqrt{2}, 2\sqrt{2}), \quad \mathbf{u}_{16} = -\mathbf{u}_{14}, \quad \mathbf{u}_{17} = -\mathbf{u}_{15}.$$

These velocities are illustrated respectively to the left and right of Figure 1. Writing $(i,j;k,l)$ for each admissible collision between speeds $\mathbf{u}_i, \mathbf{u}_j$ with outcome $\mathbf{u}_k, \mathbf{u}_l$, the collisions in the coarse model are presented in Table 1 and classified according to the effective cross-section. Similarly, the additional collisions in the fine model can be found in Table 2. A quick examination of the set of collisions shows that for each pair (i,j), only one non-trivial outcome exists. It therefore suffices to write $p_{ij}^{ij} = p_{ji}^{ij} = 1/4$, $p_{kl}^{ij} = p_{lk}^{ij} = 1/4$ for each listed collision $(i,j;k,l)$, $p_{kl}^{ij} = 0$ when the collision $(i,j;k,l)$ is physically inadmissible, and then apply the symmetries $(i) - (vi)$ to derive the complete set of transition probabilities. For the extended model, we take $\Omega_{kl}^{ij} = \Omega_{lk}^{ij} = 1$ when $(i,j;k,l)$ belongs to Table 2 and set $\lambda^{ij} \equiv \lambda$ equal for all (i,j). It is clear that the process leading from the coarse to the fine model could be repeated indefinitely, thus producing a large hierarchy of 2-D DVMs.

TABLE 1. List of collisions in coarse models.

collision type	2-D collisions	1-D collisions
type 1	$(1,3;2,4), (6,8;7,9)$	$(4,5;6,6)$
type 2	$(1,2;5,6), (2,3;5,7),$ $(3,4;5,8), (1,4;5,9)$	$(1,1;3,4), (1,2;3,6),$ $(2,2;3,5)$
type 3	$(3,6;1,7), (3,9;1,8),$ $(4,6;2,9), (4,7;2,8)$	$(2,4;1,6), (2,6;1,5)$

TABLE 2. Additional collisions in fine models.

collision type	2-D collisions	1-D collisions
type 4	$(10,12;11,13), (14,16;15,17)$	$(9,10;11,11)$
type 5	$(6,9;5,10), (6,7;5,11),$ $(7,8;5,12), (8,9;5,13)$	$(4,6;3,7), (5,6;3,8)$
type 6	$(10,11;5,14), (11,12;5,15),$ $(12,13;5,16), (10,13;5,17)$	$(7,7;3,9), (7,8;3,11),$ $(8,8;3,10)$
type 7	$(12,14;15,10), (12,17;16,10),$ $(13,14;11,17), (13,15;11,16)$	$(8,9;7,10)$

EXAMPLE 3.5. We now describe a hierarchy of 1-D DVMs obtained by an appropriate projection of the previous 2-D hierarchy. As pointed out by Beale [**D**],

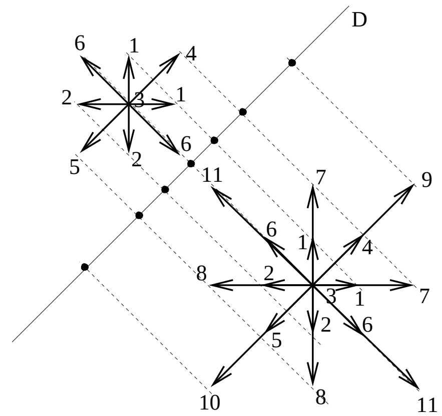

FIGURE 2. 1-D projection of coarse and fine models onto the $\mathbf{D} = (1,1)$ axis. The numbers indicate the velocities in 1-D onto which the 2-D velocities are projected.

the key is to identify in the 1-D projection only those 2-D particles that (1) have the same 1-D projected velocity, (2) have collisions that are symmetrical in 2-D with respect to the axis projection. Under these conditions, the orthogonal projection onto the (arbitrary) axis $\mathbf{D} = (1,1)$ leaves us with velocities (see Figure 2)

$$v_1 = 1, \quad v_2 = -1, \quad v_3 = 0, \quad v_4 = \sqrt{2}, \quad v_5 = -\sqrt{2}, \quad v_6 = 0. \tag{3.4}$$

where the following pairs of 2-D particles have been identified :

$$\{\mathbf{u}_1, \mathbf{u}_2\} \longrightarrow v_1, \qquad \{\mathbf{u}_3, \mathbf{u}_4\} \longrightarrow v_2, \qquad \{\mathbf{u}_7, \mathbf{u}_9\} \longrightarrow v_6,$$
$$\{\mathbf{u}_5\} \longrightarrow v_3, \qquad \{\mathbf{u}_6\} \longrightarrow v_4, \qquad \{\mathbf{u}_8\} \longrightarrow v_5.$$

The masses are therefore $\nu_1 = 2, \nu_2 = 2, \nu_3 = 1, \nu_4 = 1, \nu_5 = 1, \nu_6 = 2$. Now, we assign the transition probabilities in the 1-D model to be those of *one of it's representatives* in the 2-D model. For example, if one wants to know the transition probability p_{KL}^{IJ} in the 1-D model, then we set it equal to the transition probability p_{kl}^{ij} from the 2-D model where $\mathbf{u}_i, \mathbf{u}_j, \mathbf{u}_k, \mathbf{u}_l$ were projected respectively onto v_I, v_J, v_K, v_L. From the first column of Table 1, we deduce the set of collisions in the 1-D model presented in the second column.

For the fine 1-D model, the projection of the 2-D model leads to the additional velocities

$$v_7 = \sqrt{2}, \quad v_8 = -\sqrt{2}, \quad v_9 = 2\sqrt{2}, \quad v_{10} = -2\sqrt{2}, \quad v_{11} = 0, \tag{3.5}$$

the additional masses $\nu_7 = 2, \nu_8 = 2, \nu_9 = 1, \nu_{10} = 1, \nu_{11} = 2$, and the projections

$$\{\mathbf{u}_{10}, \mathbf{u}_{11}\} \longrightarrow v_7, \qquad \{\mathbf{u}_{12}, \mathbf{u}_{13}\} \longrightarrow v_8, \qquad \{\mathbf{u}_{15}, \mathbf{u}_{17}\} \longrightarrow v_{11}$$
$$\{\mathbf{u}_{14}\} \longrightarrow v_9, \qquad \{\mathbf{u}_{16}\} \longrightarrow v_{10}.$$

The resulting set of collisions is given in the second column of Table 2.

4. Numerical results

In this section, we test the numerical efficacy of the error estimator developed in [**A**] and stated in Section 2. For initial data that is equal for both the coarse and fine models, the *efficacy* is the quantity

$$\eta(t) := \frac{\int_0^t \|R(\mathbf{f})\|(\tau)\mathrm{d}\tau}{\sum_i \bar{\nu}_i \|f_i(t) - \bar{f}_i(t)\|_{L^1}}, \tag{4.1}$$

which one would like to be not too large, largely independent of time, and preferably equal to 1. The numerical experiments are applied to the model described in Section 3 and the main parameters we examine are the total mass of the initial data and the distance between the two models $\lambda^{ij} := \lambda$, first presented in Lemma 3.2. We show that the error estimate is, quite surprisingly, largely independent of the size of the initial data, but that λ must be small for the efficacy to be close to 1.

We solve the PDEs (1.1) and (1.2) in a bounded domain $\Omega = [-10, 10]$ and over a time interval $[0, 20]$ that are both sufficiently large that the solution has reached it's asymptotic profile, i.e. it begins to look like N distinct waves travelling at the characteristic speeds $v_1, \ldots, v_N$ [**D**]. The boundary conditions are absorbing for those characteristics that are outgoing and fixed equal to the initial data $f_{i,0}|_{\partial\Omega}$ for the incoming characteristics. The constants A^{ij}_{kl} use the mean free path $\varepsilon = 1$ and the constant $C = 1$. The initial data $f_{i,0} = \bar{f}_{i,0}, i = 1, \ldots, N$, is obtained as follows. We pick $N = 6$ velocities $v_1^* = -2, v_2^* = -1.2, v_3^* = -0.4, v_4^* = 0.4, v_5^* = 1.2, v_6^* = 2.0$, $N = 6$ points $x_1^* = -5, x_2^* = -3, x_3^* = -1, x_4^* = 1, x_5^* = 3, x_6^* = 5$, and then compute

$$f_{i,0}(x) = A_0 \sum_{j=1}^{N} \mathrm{erf}(x - x_j^*) \cdot \exp\big(-(v_i - v_j^*)^2\big). \tag{4.2}$$

and $\bar{f}_{i,0} \equiv 0$ when $i > N$. The positive parameter A_0 is proportional to the total mass in L^1. The initial data is formed of 7 humps located at x_j^* and concentrated around velocities v_j^*.

The DVMs (1.1) and (1.2) are solved numerically using a splitting of the collision and transport terms at each timestep Δt. For the collision step, the time-dependent ODE is solved using a Runge-Kutta method of order 4 with $h = \Delta t/10$. In the integrals involved in the definition of the efficacy are estimated using Simpson's method. The code was shown to converge to first order, which was sufficient for its intended use.

In the first graph, on the left of 3, we show the true error and the error estimators as functions of t when $A_0 = 0.1$ and $\lambda = 0.25$. This result confirms that the error estimator provides an accurate measure of the divergence in time of the solutions to (1.1) and (1.2). On the right of Figure 3, we show the efficacy (4.1) as a function of t for $A_0 = 0.1$ and $\lambda = 0.75, 0.25, 0.125, 0.0625$. The graph shows the estimator is reasonable even for very different DVMs. Numerical results not presented showed that for fixed $\lambda = 0.25$ and $A_0 = 0.8, 0.4, 0.2, 0.1$, the curves of efficacy were essentially identical, which is somewhat surprising given the hypothesis in Theorem 2.3. Taken together, these numerical results indicate that the error estimator could be used for adaptive error estimation. Such an application is the subject of ongoing research [**B**].

References

[A] K. Assi and M. Laforest. Modeling error in L^1 for a hierarchy of 1-D discrete velocity models. 2008. Submitted to Trans. Theory and Stat. Phys., 26 pages.

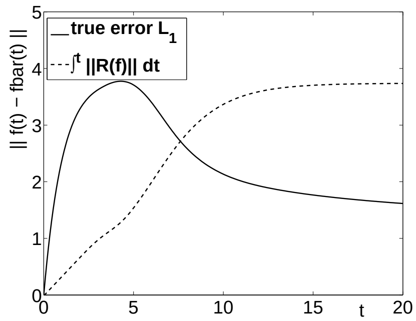

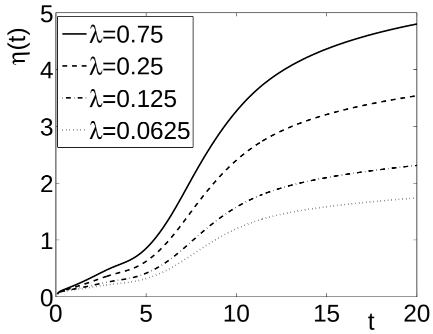

FIGURE 3. On the left, the graph presents the true error in L^1 and the error estimator as functions of time. On the right, the efficacity is presented as a function of time for different values of λ.

[B] K. Assi, M. Laforest and E. M. Zaoui. An adaptive version of the Random Discrete Velocity Model. Technical report, 2008. In preparation.

[C] K. C. Assi. *Version adaptative d'un modèle à vélocité discrète pour l'équation de Boltzmann*. M.Sc. thesis (in french), École Polytechnique de Montréal, 2008.

[D] J. T. Beale. Large time behavior of discrete velocity Boltzmann equations. *Commun. Math. Phys.*, 106:659–678, 1986.

[E] A. V. Bobylev and C. Cercignani. Discrete velocity models without nonphysical invariants. *J. Stat. Phys.*, 97(3):677–686, 1999.

[F] J.-M. Bony. Solutions globales bornées pour les modèles discrets de l'équation de Boltzmann, en dimension 1 d'espace. In *Journées équations aux dérivées partielles (Saint Jean de Monts, 1987)*, volume XVI, page 10. 1987.

[G] R. Gatignol *Théorie cinétique des gaz à répartition discrète de vitesses*, volume 36 of *Lecture Notes in Physics*. Springer-Verlag, Berlin, New York, 1975.

[H] S. Y. Ha and A. E. Tzavaras. Lyapunov functionals and L^1-stability for discrete velocity boltzmann equations. *Comm. Math. Phy.*, 239:65–92, 2003.

[I] R. Illner and S. Rjasanow. Numerical solution of the Boltzmann equation by random discrete velocity models. *Eur. J. Mech. B.*, 13(2):197–210, 1994.

[J] L. Mieussens. Discrete-velocity models and numerical schemes for the Boltzmann-BGK equation in plane and axisymmetric geometries. *J. Comp. Phys.*, 162(2):429–466, 2000.

[K] B. T. Nadiga. An adaptive discrete-velocity model for shallow water equations. *J. Comp. Phys.*, 121:271–280, 1995.

[L] T. Nishida and M. Mimura. On the Broadwell model of the Boltzmann equation for a simple discrete velocity gas. *Proc. Japan. Acad.*, 50:812–817, 1974.

[M] L. Tartar. Existence globale pour un systéme hyperbolique semi linéaire de la théorie cinétique des gaz. In *Séminaire Goulaouic-Schwartz (1975-1976), Équations aux dérivées partielles et analyse fonctionnelle*. Centre Math. Palaiseau: École Polytechnique, 1976. Exp. 1, 11 pp.

DÉPARTEMENT DE MATHÉMATIQUES ET GÉNIE INDUSTRIEL, ÉCOLE POLYTECHNIQE DE MONTRÉAL, C.P. 6079, SUCC. CENTRE-VILLE, MONTRÉAL, QUÉBEC, CANADA H3C 3A7

E-mail address: kondo-claude.assi@polymtl.ca

DÉPARTEMENT DE MATHÉMATIQUES ET GÉNIE INDUSTRIEL, ÉCOLE POLYTECHNIQE DE MONTRÉAL, C.P. 6079, SUCC. CENTRE-VILLE, MONTRÉAL, QUÉBEC, CANADA H3C 3A7

E-mail address: marc.laforest@polymtl.ca